

Influence of Different Reynolds Numbers on Aerodynamic Losses in Low Pressure Turbines

Yue Long and Wang Yun-fei*

School of Transportation and Vehicle Engineering, Shandong University of Technology, 255049, Zhangdian district, Zibo city, Shandong province, China.

*Corresponding author email id: wangyunfei@sdut.edu.cn

Date of publication (dd/mm/yyyy): 22/06/2021

Abstract – In order to understand the influence of aerodynamic losses in low-pressure turbines with different Reynolds numbers in more detail, the Reynolds average method (RANS) was adopted to calculate the flow fields in low-pressure turbines with Reynolds numbers of 0.6×10^5 , 1.0×10^5 , 2.0×10^5 and 3.0×10^5 . The results show that the numerical simulation method adopted in this paper can describe the internal flows in low-pressure turbines more accurately. Under the low Reynolds number condition, the flow in the endzone is more complex, and the flow field parameters vary greatly at different blade heights, and the parameters tend to be stable at $z/h = 0.5$. The larger Reynolds number can reduce the size and strength of the passage vortex, the transverse pressure behind the blade suction surface, the total pressure loss behind the gate, the width of the wake region and the velocity loss, so as to reduce the aerodynamic loss of the whole blade.

Keywords – Reynolds Number, Total Pressure Loss, Channel Vortex, Numerical Simulation.

I. INTRODUCTION

The Reynolds number of an aeroengine varies with the change of flight altitude and speed, and the internal flow field structure of the low-pressure turbine in the engine is very different from the design state at different Reynolds numbers, and its aerodynamic characteristics show a nonlinear downward trend at low Reynolds numbers. Therefore, it is necessary to master the influence of different Reynolds numbers on aerodynamic losses of low-pressure turbine.

The working Reynolds number of the low-pressure turbine is within the range of 0.4×10^5 to 5.0×10^5 , which is the lowest level in the whole aero-engine. Hourmouziadis [1] pointed out that the lower the Reynolds number is, the more likely laminar flow separation is to occur, which changes the flow in the boundary layer on the suction surface of blades, thus further affecting the profile loss and secondary flow loss in the end zone. Woinowsky-Krieger et Al [2] conducted an experiment on a single-stage transonic high pressure turbine by changing the Reynolds number from 0.32×10^5 to 2.5×10^5 . The experiment found that when the Reynolds number was lower than 1×10^5 , the turbine stage efficiency decreased significantly, and when the Reynolds number was higher than this value, the turbine stage efficiency was relatively stable. Marks et Al [3] conducted a similar experiment on the low-speed cascade test bench, the experimental results showed that with the Reynolds number gradually increasing from 0.3×10^5 to 1.0×10^5 , the passage vortices migrated upstream, and the total pressure loss behind the cascade, the width of wake region, as well as the size and intensity of the passage vortices all decreased. A large number of studies [4-7] have shown that different Reynolds numbers have different influences on the boundary layer of low-pressure turbines. At low Reynolds numbers, the suction surface boundary layer is easier to separate. The Reynolds number changes the development of secondary flows in the end zone by affecting the thickness and state of the boundary layer of the inlet flow. But, Satta et Al [8] studied the flow field behind the gate under two operating conditions of 1×10^5 and 3×10^5 , and finally found that the intensity and loss of secondary flow in the end-zone under high Reynolds number condition were signif-

-icantly higher than that under low Reynolds number condition.

Although the influence of Reynolds number has been explained by various research methods, the influence of Reynolds number on turbine flows is extremely complex. The current research has not elaborated on the influence mechanism and variation rules of different Reynolds numbers, and more detailed research and summary are still needed. On the basis of the existing research, the flow field of low-pressure turbines in four working conditions of Reynolds number from 0.6×10^5 to 3.0×10^5 is numerically simulated in this paper. The influence of Reynolds number on the variation of aerodynamic loss and the source of aerodynamic loss is analyzed in detail, which provides a reference for the design and improvement of low-pressure turbines.

II. NUMERICAL SIMULATION METHOD

Figure 1 shows the T106A cascade end plane grid distribution and local grid amplification figure around the leading edge and trailing edge, the distance from inlet to the the blade leading edge is $1.0 C_{ax}$, the distance from outlet of plane cascade to trailing edge is $1.6 C_{ax}$, high computational domain is half a leaf, set up the plane of symmetry, in two and a half high calculation domain simulation of the whole leaf, improve the efficiency of

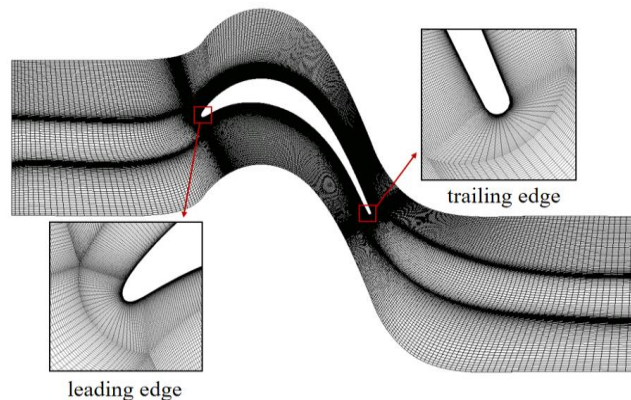


Fig. 1. Computational grid for the cascade, zoomed view of leading edges and trailing edges.

software calculation. x , y and z are the circumferential, flow and spanwise directions respectively. C_{ax} is taken as the reference length to dimensionless the dimensions of the calculation domain. After dimensionless, the circumferential, flow and spanwise dimensions are 0.94, 3.6 and 2 respectively, and there are 127 nodes in circumferential direction, 938 nodes in flow direction and 100 nodes in spanwise direction. The grid number of global computing domain is 8.02 million.

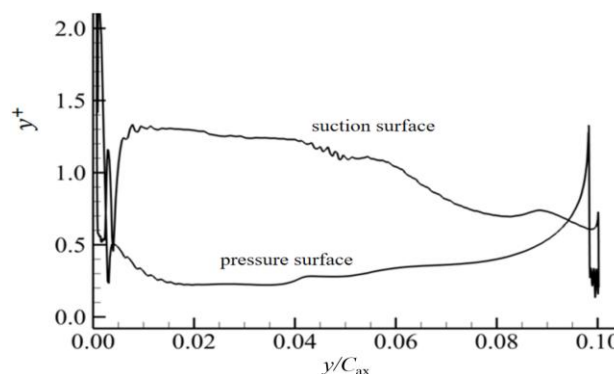


Fig. 2. The variation of y^+ along the flow direction.

Fig. 2 shows the y^+ distribution of the first layer grid on the cascade surface along the normal direction. Through comparative analysis of the experiment, it can be seen that y^+ on the cascade surface increases with the increase of Reynolds number, so only the y^+ distribution in the condition that Reynolds number is 3.0×10^5 is given. In order to reduce the the influence of inlet turbulivity on flow uncertainty, so the inlet turbulivity was set as 0.96% to ensure the reliability of the calculation results.

III. ANALYSIS OF CALCULATION RESULTS

Firstly, the calculation results were checked and compared with the experimental results and DNS results in reference [9, 10] for $Re_{2th} = 0.6 \times 10^5$ condition. 1, 2 represent upstream and downstream respectively, and th represents outlet. Fig. 3 shows the distribution of static pressure coefficient on blade surface at 50% blade height, and the static pressure coefficient is defined as $C_p = \frac{p - p_2}{p_{t1} - p_2}$

In this formula, p is the static pressure value of cascade surface; p_{t1} is the total inlet pressure; p_2 is the outlet static pressure. Obtained from figure 2, RANS computation results, experimental results and the DNS results were given in the literature, we can clearly observed that there is a platform in the graph line at the back of the suction surface, the boundary layer separation, quickly reduce the blade surface gas velocity, then the line shock occurs, the reason is in the separation of free shear layer transition happens, after transition, the pressure increases rapidly and finally reaches the pressure value of the trailing edge.

Fig. 4 shows the distribution of the total pressure loss coefficient along the circumferential direction of the cascade downstream distance of 40% chord length, and the total pressure coefficient is defined as $\Omega = \frac{p_{t1} - p_{t2}}{p_{t1} - p_2}$

In this formula: p_{t2} is the total pressure at the exit after spreading average. The circumferential distance between two adjacent blades was normalized, and $y^* = 0$ was used to represent the suction surface side, and $y^* = 1$ was used to represent the pressure surface side. By comparing the above two parameters with the experimental and DNS results, it is concluded that the calculated results were basically consistent with the actual situation. This calculation model could be used for calculation and analysis.

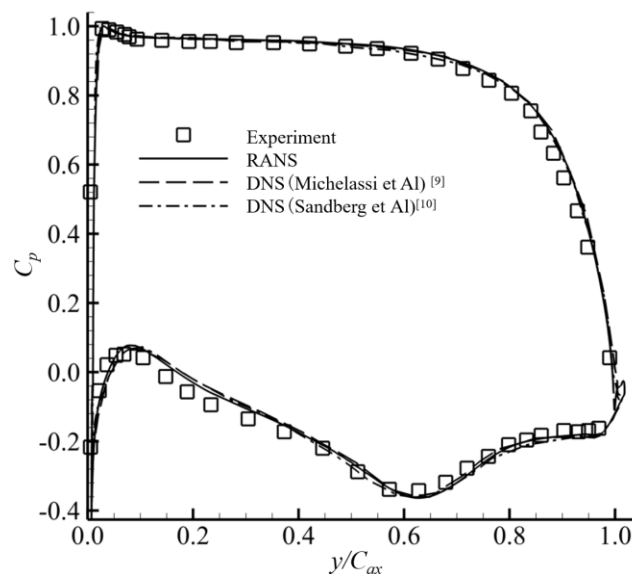


Fig. 3. Static pressure coefficient at 50% height.

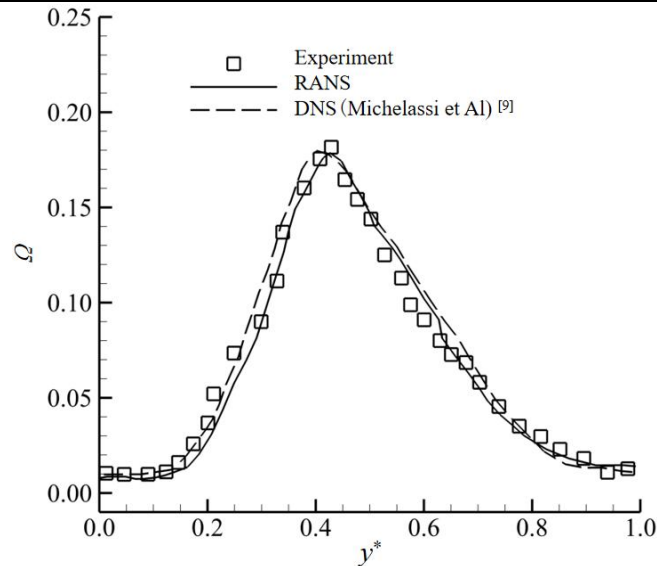


Fig. 4. Distribution of total pressure loss coefficient.

Fig. 5 shows the variation of total pressure loss coefficients in different flow sections with the direction of blade height in the conditions of different Reynolds numbers. We can clearly observe that the total pressure loss of the airflow is mainly concentrated near the end zone. At $y/C_{ax}=0.25$, the total pressure loss in different Reynolds number conditions is small. Here, the vortex system has a simple structure, and its influence on flow loss is mainly concentrated near the endwall. However, due to the strong viscosity of low Reynolds number, we can also find that the total pressure loss slightly increases with the decrease of Reynolds number. At $y/C_{ax}=0.5$, the total pressure loss in different Reynolds number conditions has obvious difference. It is mainly concentrated in the area below $z/h=0.06$. The smaller the Reynolds number is, the higher the total pressure loss will be, the influence is the largest at $z/h=0.04$. Here, the total pressure loss is at its peak, and the passage vortex has already played its role, rising and growing continuously, which plays a significant role in the flow loss.

However, at $y/C_{ax}=0.75$, the passage vortex continues to rise, the flow loss continues to increase, and the influence area gradually expands. The loss area is mainly concentrated in the zone of $z/h=0.06-1.08$. The smaller the Reynolds number is, the greater the total pressure loss is, and the maximum influence is at the position of $z/h=0.06$, and the total pressure loss is at the peak. The smaller the Reynolds number is, the higher the peak height is. After $y/C_{ax}=1.00$, the passage vortex continues to rise, the flow loss continues to increase, and the influence range gradually expands. There will be a peak point of the total pressure loss coefficient. The smaller the Reynolds number, the larger the peak value of the peak point and the higher the height. This is the core region of the passage vortex. The smaller the Reynolds number is, the pressure loss of the passage vortexes is at the peak. The passage vortexes have played a role and are constantly rising and growing, which plays a non-negligible role in the flow loss. The higher the intensity of passage vortex, a substantial increase of the blade aerodynamic losses, the growth of the Reynolds number of peak value of the total pressure loss has significant inhibitory effect, the effect of Reynolds number below the peak point is not big, but above the peak point of the area, the smaller the Reynolds number, the larger the total pressure loss, and the growth rate of total pressure loss increases with the reduction of Reynolds number is growing. Take a look at Figure 5, it can be seen that the growing Reynolds number has a restraining effect on the height and intensity in the core area of the passage vortex and total pressure loss.

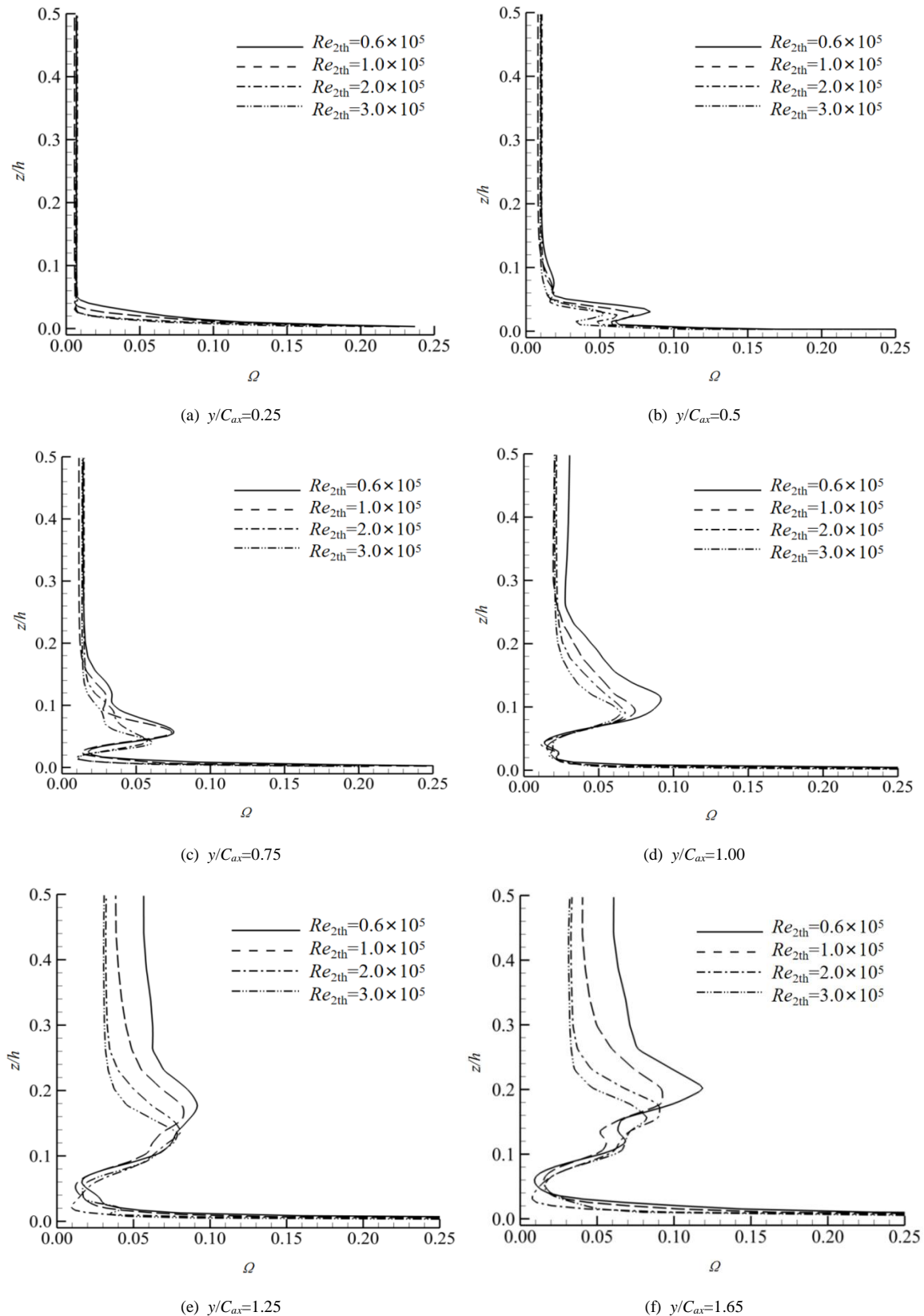


Fig. 5. Distribution Distribution along the leaf height of total pressure loss coefficient for different flow cross sections under various Reynolds numbers.

In order to analyze the influence of different Reynolds number conditions on the flow loss in the channel in more detail, four sections perpendicular to the flow direction were intercepted in the calculation domain, as

shown in Fig. 6. Fig. 7 shows the distribution cloud map of the total pressure loss coefficient on each section. The total pressure loss caused by channel vortices varies greatly in different Reynolds number conditions, and the obvious loss is greater in low Reynolds number conditions. As can be seen from Fig. 7, the influence of Reynolds number on aerodynamic losses in the passage is mainly concentrated in the area above the passage vortex and close to the suction surface. Compared with the 4 images of the cross section (c, g, k, o) of $y/C_{ax} = 1.00$ in Fig. 7, the loss is large in section (c, g) because it is in the separation area behind the suction surface. Passage vortex above total pressure loss near the suction surface area for the most part of the whole passage vortex loss, and with the increase of Reynolds number, total pressure loss in the region are in decline in size and scope, the structure of the passage vortex undermined its separation bubble around, around the blade near the blade gases involved, decrease the total pressure loss near the blade. With the increase of

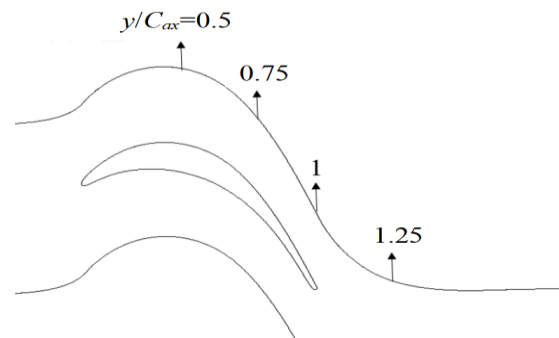
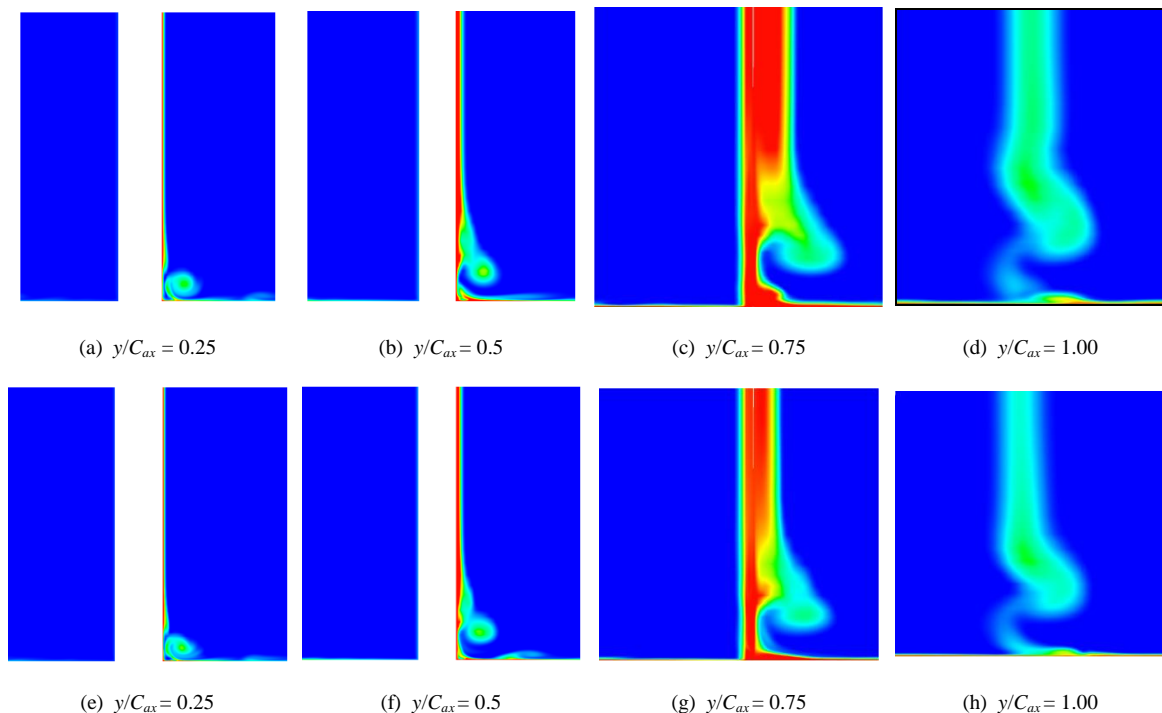


Fig. 6. Sketch map of 4 cross sections along the flow direction.

Reynolds number, the loss of the end face angle region decreases, and the volume of the passage vortex also decreases, but the Reynolds number has little effect on the radial position of the core of the passage vortex. In the cross section of $y/C_{ax} = 1.00$, the passage vortex continues to develop in the downstream region away from the cascade, and there is still an obvious loss area on the upper and lower endwalls of the passage vortex, but both of them have a decreasing trend with the increase of Reynolds number.



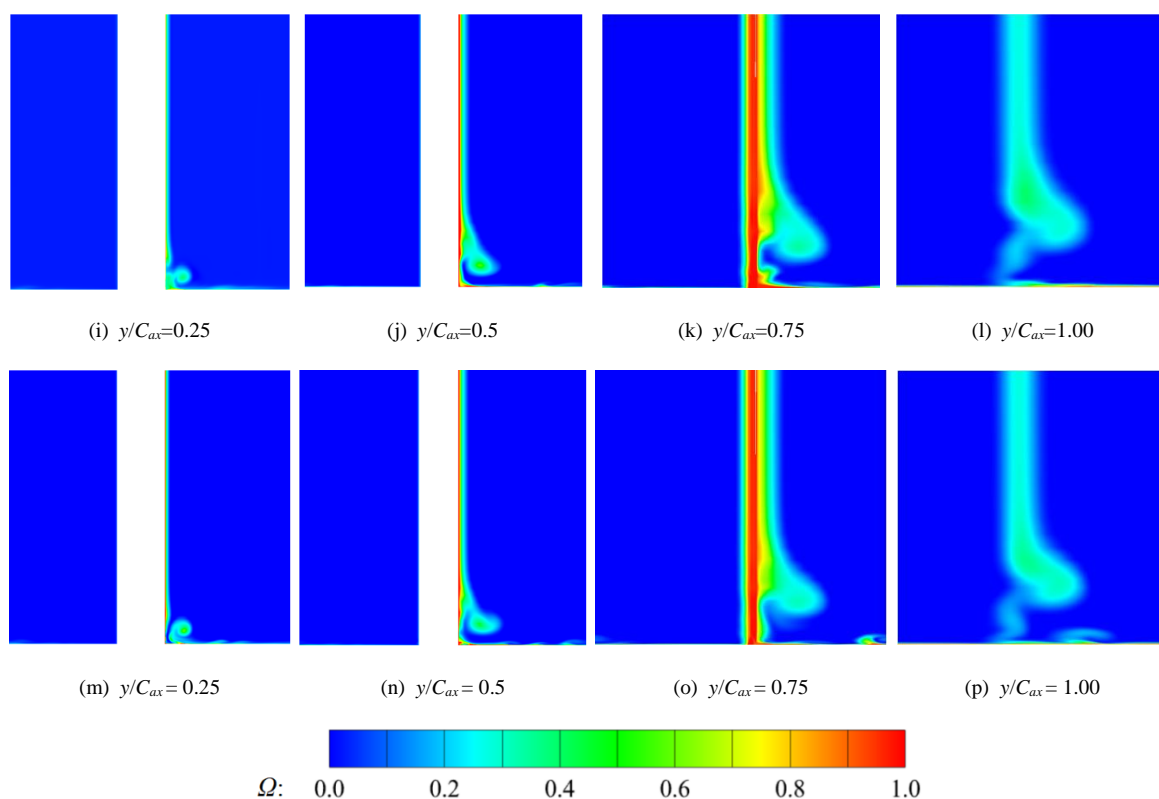


Fig. 7. Cloud map of total pressure loss coefficient of different flow sections at different Reynolds numbers.

ACKNOWLEDGMENT

This work was supported by the project ZR2020QE190 supported by Shandong Provincial Natural Science Foundation and the Scientific Research Foundation of Shandong University of Technology.

REFERENCES

- [1] Hourmouziadis J. (1989). Aerodynamic design of low pressure turbines. AGARD lecture series 167.
- [2] Woinowsky-Krieger M, Lavoie JP, Vlasic EP, Moustapha SH (1999). Off-Design performance of a single-stage Transonic Turbine. *Journal of Turbomachinery*, 121(2): 177-183.
- [3] Marks, C. R., Sondergaard, R., Bear, P. S., Wolff, M. Reynolds number effects on the secondary flow of profile contoured low Pressure Turbines. AIAA Paper, 2016-0114.
- [4] Montomoli F, Hodson H, Haselbach F(2010). Effect of Roughness and unsteadiness on the performance of a new low pressure Turbine Blade at low reynolds numbers. *Journal of Turbomachinery*, 132(3): 031018.
- [5] Pichler Richard et al (2019). Large-eddy simulation and RANS analysis of the end-wall flow in a linear low-pressure Turbine Cascade, Part I: Flow and Secondary Vorticity Fields Under Varying Inlet Condition [J]. *Journal of Turbomachinery*, 141(12)
- [6] Mahallati A, Mcauliffe B R, Sjolander S , et al(2007). Aerodynamics of a low-pressure Turbine Airfoil at Low Reynolds Numbers- Part I: Steady Flow Measurements. *Journal of Turbomachinery*, 135(1):011010.
- [7] Cui Jiahuan and Tucker Paul(2017). Numerical study of purge and secondary flows in a low-pressure Turbine [J]. *Journal of Turbomachinery*, 139(2)
- [8] Satta F, Simoni D, Ubaldi M, et al. Profile and secondary flow losses in a high-lift LPT blade cascade at different Reynolds numbers under Steady and Unsteady Inflow Conditions. *Journal of Thermal Science*, 2012(06): 3-11.
- [9] Michelassi V, Chen Liwei, Pichler R, et al(2015).Compressible direct numerical simulation of low-pressure turbines-part ii: effect of inflow disturbances[J]. *Journal of Turbomachinery*, 137(7): 071005.
- [10] Sandberg R D, Pichler R, Chen L(2012).Assessing the sensitivity of turbine cascade flow to inflow disturbances using direct numerical simulation[C]//Proceedings of the 13th International Symposium for Unsteady Aerodynamics, Aeroacoustics and Aeroelasticity in Turbomachinery (ISUAAAT). Tokyo, Japan: ISUAAAT Scientific Committee.

AUTHOR'S PROFILE



First Author

Yue Long, He's a graduate student, Shandong University of Technology, Shandong. His Research Area: evolution mechanism of internal flow field in turbomachinery, complex flow mechanism of boundary layer transition and flow control.



Second Author

Wang Yun-fei, He's a lecturer, Shandong University of Technology, Shandong. His Research Area: evolution mechanism of internal flow field in turbomachinery, complex flow mechanism of boundary layer transition and flow control. He has 10 years of research experience.